Electronic Supplementary Material (ESI) for Nanoscale.

[Supplementary Information]

Impact of Thermally Dead Volume on Phonon Conduction along Silicon Nanoladders

Woosung Park,[a,] Joon Sohn,[b] Giuseppe Romano,[c] Takashi Kodama,[a] Aditya Sood,[a,d] Joseph S. Katz,[a,b] Brian S. Y. Kim,[e] Hongyun So,[f] Ethan C. Ahn,[g] Mehdi Asheghi,[a] Alexie M. Kolpak,[c] and Kenneth E. Goodson[a,]**

[a] Department of Mechanical Engineering, [b]Department of Electrical Engineering, Stanford University, Stanford, California 94305, USA

[c] Department of Mechanical Engineering, Massachusetts Institute of Technology, Cambridge, Massachusetts 02139, USA

[d] Department of Materials Science and Engineering, [e] Geballe Laboratory for Advanced Materials, Stanford University, Stanford, California 94305, USA

[f]Department of Mechanical Engineering, Hanyang University, Seoul, 04763, South Korea

[g]Department of Electrical and Computer Engineering, The University of Texas at San Antonio, 1 UTSA Circle, San Antonio, TX 78249, USA

Uncertainty analysis

We estimate the experimental uncertainty by adding up the individual error contributions of each component in quadrature:

$$\left.\frac{\Delta k}{k}\right|_{Total} = \sqrt{\left(\left.\frac{\Delta k}{k}\right|_{Var.1}\right)^2 + \left(\left.\frac{\Delta k}{k}\right|_{Var.2}\right)^2 \cdots} \qquad \text{(S1)}$$

where k is thermal conductivity and Var indicates sources of experimental error. The experimental error is mainly due to the uncertainty in sample dimensions, which are inherently caused by tolerances in nanofabrication and the limit in scanning electron microscope (SEM) measurements. We estimate the uncertainty in dimensions and their propagation to thermal conductivity as summarized in Table S1. The total measurements uncertainty is calculated to be less than ~7% of the thermal conductivity throughout the samples.

Table S1. Uncertainty Analysis

Samples	k ($Wm^{-1}K^{-1}$)	w_{Hole} (±5 nm) Error (%)	l_{Hole} (±5 nm) Error (%)	t (±5 nm) Error (%)	Total Error (%)
l_{Hole} = ~70 nm	~31.0	~1.3	~0.0	~6.3	~6.4
l_{Hole} = ~170 nm	~36.5	~1.4	~2.0	~6.3	~6.7
l_{Hole} = ~270 nm	~37.6	~1.9	~2.2	~6.3	~7.0
l_{Hole} = ~470 nm	~41.4	~1.8	~1.8	~6.3	~6.8
l_{Hole} = ~970 nm	~45.0	~1.7	~1.4	~6.3	~6.7
Ref. Beam w_{Beam} = ~970 nm	~50.4	-	-	~6.3	~6.3

Model comparison between direct calculations of Boltzmann transport equation and predictions using a ray-tracing method with Monte Carlo integration

We compare two modeling approaches: one obtained through direct calculations of the Boltzmann transport equation and the other using a ray-tracing method with Monte Carlo integration. As the details of the direct calculations are explained in the main text, we mainly describe the method of model prediction using a ray-tracing method. We model phonon transport in the nanostructures samples using Eq. (1), recasting here

$$k = \int_0^\infty S_\Lambda(\Lambda) f(\Lambda) d\Lambda \tag{S2}$$

where *f* is the differential phonon MFP distributions for bulk silicon, S_Λ is the phonon suppression function, and Λ is an integration variable for phonon MFP in bulk silicon. Using Matthiessen's approximation, the suppression function S_Λ can be obtained using a ratio of mean free paths (MFPs) in samples to those in bulk material[1]

$$S_\Lambda(\Lambda_{bulk}) = \left(1 + \Lambda_{bulk}/\Lambda_{boundary}\right)^{-1} \tag{S3}$$

where Λ_{bulk} and $\Lambda_{boundary}$ are MFPs due to internal and boundary scatterings, respectively. We obtain Λ_{bulk} from *ab initio* calculations.[2] We use the ray-tracing method with Monte Carlo integration to determine $\Lambda_{boundary}$ for the three dimensional nanoladder structures.[3, 4] A thousand phonon particles are generated in a computational domain with randomly selected initial position and orientation, and the particles travel ballistically until they reach boundaries. The phonons scatter diffusely from the boundaries following Lambert's cosine law.[5] The phonon trajectories are traced until passing 100 cells. The prediction using the ray-tracing model is shown in Figure S1 with experimental results and direct BTE calculations. Both the direct BTE calculations and the model using the ray-tracing method predict the thermal conductivity for the silicon nanoladders as well as two straight beams with w_{Neck} = 70 nm and 970 nm within ~11%.

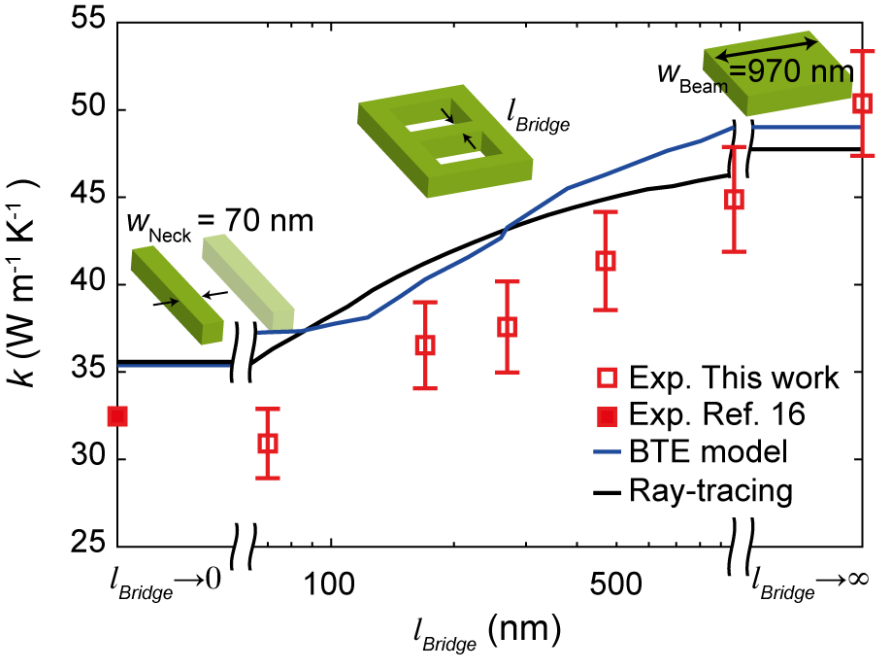

Figure S1. Thermal conductivity of the nanoladders with a function of spacing l_{Bridge} with two models: one from direct calculations of the Boltzmann transport equation and the other using a ray-tracing method, which are in blue and black solid lines, respectively.

Theoretical validation for the use of a straight beam with a cross-section of ~78 nm thickness and ~ 65 nm for the limiting case $l_{\text{Bridge}} \rightarrow 0$

In the present work, we use the thermal conductivity of a straight beam with a cross-section of ~78 nm thickness and ~ 65 nm for the limiting case $l_{\text{Bridge}} \rightarrow 0$, which is the counterpart with ~75 nm thick and 70 nm wide cross-section. Based on Equation (S2) and (S3), the impact of boundary scattering is estimated using $\Lambda_{boundary}$, which is given by

$$\Lambda_{Boundary} = \frac{3w}{4}\left(ln2(h/w) + \frac{w}{3h} + 1/2\right) \quad \text{(S4)}$$

where w and h are width and thickness of a cross-section, respectively.[4] The $\Lambda_{Boundary}$ for both beams, one with ~ 65 nm width and ~78 nm thickness and the other with ~70 nm width and ~75 nm thickness, are ~81 nm and ~83 nm, respectively. This difference results in a ~1% difference of thermal conductivity.

Impact of a thermally dead volume in diffusive transport regime

We display heat flux maps for nanoladders in both quasi-ballistic and diffusive transport regimes in Figure S2. It is noteworthy that a significant volume of bridges minimally contributes to net heat transfer in both transport regimes. We note that the heat flux map for diffusive transport is obtained by calculating Boltzmann transport equations for the case of bulk MFP = 2 nm, where the impact of boundary scattering is negligible.

To quantify the impact of the bridges in diffusive transport regime, we calculate thermal conductance for the nanoladders, and the conductance C is given by

$$C = \frac{q}{\Delta T} \tag{S4}$$

where q is a net heat flux along the structures, and ΔT is a temperature difference across the structures. Thermal conductance indicates an ability of material to transfer heat, including geometric components. We normalize the conductance with twice that of a straight beam with w_{Neck} = 70 nm, which corresponds to free line-of-sight, and the plot is shown in Figure S3. We observe that the bridges decreasingly contribute to net heat transfer with decreasing spacing between adjacent rectangular holes in both ballistic and diffusive transport regimes. This negligible contribution indicates that the bridges serve largely as a dead space even in the diffusive transport regime. The difference between these conductances is attributed to the ballistic effect in the nanoladders. We compare the thermal conductances in quasi-ballistic regime, and these values are normalized with that of a straight beam with suppressed thermal conductivity due to ballistic effects.

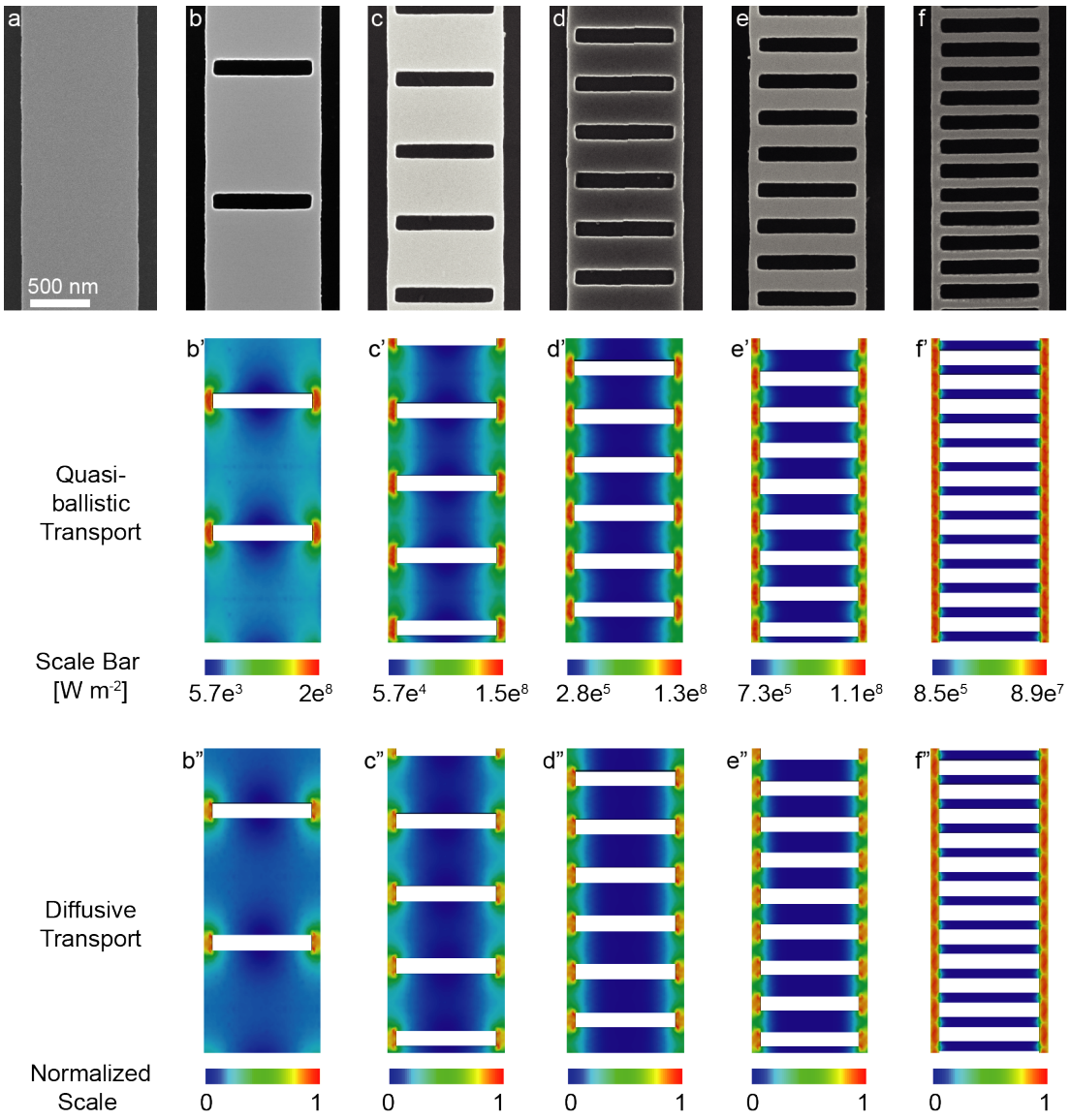

Figure S2. (a-f) Scanning Electron Microscopy (SEM) images of (a) a reference beam, l_{Bridge} = (b) 970 nm, (c) 470 nm, (d) 270 nm, (e) 170 nm, and (f) 70 nm. (g) (b'-f') Quasi-ballistic and (b"-f") diffusive heat flux maps that are obtained by solving three-dimensional BTE, and the scale bars are shown below each map. The length scale bar in (a) is shared through (a-f), (b'-f'), and (b"-f").

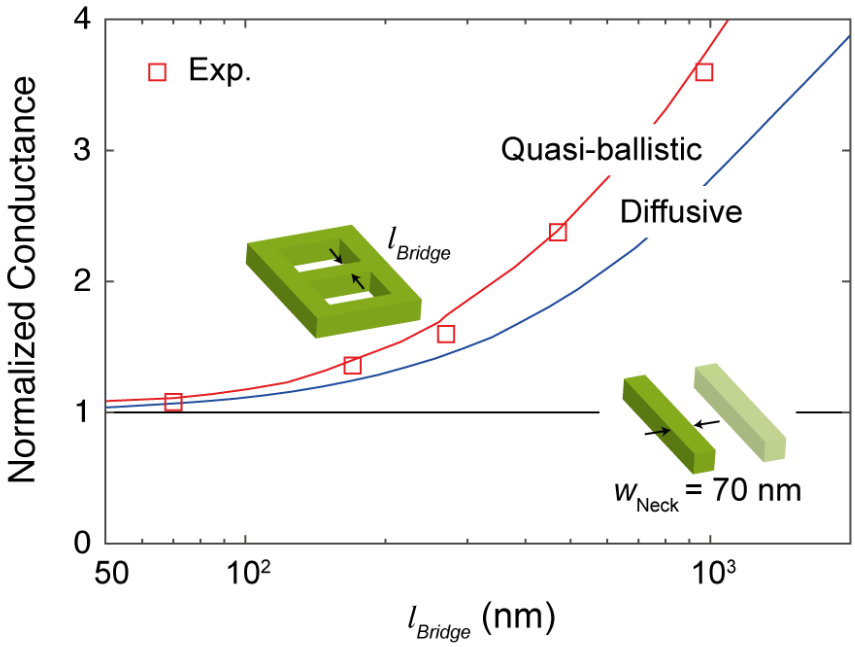

Figure S3. Normalized thermal conductance as a function of spacing l_{Bridge}. Quasi-ballistic and diffusive transports are shown in red and blue solid lines, respectively. The black solid line indicates the thermal conductance of two straight beam with w_{Neck} = 70 nm, which is equivalent to unobstructed line-of-sight channels in the nanoladders.

1. F. Yang and C. Dames, *Phys. Rev. B*, 2013, **87**, 35437-35443.

2. K. Esfarjani, G. Chen and H. T. Stokes, *Phys. Rev. B*, 2011, **84**, 085204.

3. T. Hori, J. Shiomi and C. Dames, *Appl. Phys. Lett.*, 2015, **106**, 171901.

4. J. Lee, W. Lee, G. Wehmeyer, S. Dhuey, D. L. Olynick, S. Cabrini, C. Dames, J. J. Urban and P. Yang, *Nat. Commun.*, 2017, **8**, 14054.

5. K. Kukita and Y. Kamakura, *J. Appl. Phys.*, 2013, **114**, 154312.